Control of Neuromuscular Blockade in the Presence of Sensor Faults

João M. Lemos, *Member, IEEE*, Hugo Magalhães, Teresa Mendonça*, *Member, IEEE*, and Rui Dionísio

***Abstract*—The problem of embedding sensor fault tolerance in feedback control of neuromuscular blockade is considered. For tackling interruptions of feedback measurements, a structure based upon Bayesian inference as well as a predictive filter is proposed. This algorithm is general and can be applied to different situations. Here, it is incorporated in an adaptive automatic system for feedback control of neuromuscular blockade using continuous infusion of muscle relaxants. A significant contribution consists in the experimental clinical testing of the algorithm in patients undergoing surgery.**

***Index Terms*—Bayes inference, hybrid systems, median filter, neuromuscular blockade, outliers, physiological systems, supervisory multiple models control.**

I. Introduction

PHYSIOLOGICAL variables are associated to systems whose dynamic behavior is highly uncertain and usually time varying. Furthermore, their measurement may be unreliable and susceptible to random interruptions, due to the complexity and the indirect principles upon which they rely. "Interruptions" or "faults" are defined as situations in which the signal yielded by the sensor is, during a transient period, not related to the variable to be measured. If these measurements are used for closing a control loop, their interruptions may induce strong transients or even instability. Indeed, an interruption of measurement will be interpreted by the controller as a fake disturbance to which it will react, thereby degrading performance. Furthermore, if an adaptive controller whose identifier relies on least squares is used, controller gains may be strongly detuned since the quadratic criteria will greatly amplify high amplitude errors. Last, but not least, interruptions have an impact on safety of the patient undergoing surgery which depends on sensor measurements.

Performing estimation in the presence of small duration sensor faults, known as outliers, is an important problem in statistics [1]. Outliers are large deviations of the signal being measured, occurring only in a few percent of the observed samples, but probable enough not to be explainable by the tails of a Gaussian distribution. Since outliers are due to unknown causes and they cannot usually be modeled from first principles, one has to resort to statistical methods to tackle the problems raised by them.

The asymptotic relative efficiency of an estimator [2] is defined as the ratio between the lowest achievable variance for the estimated parameters (the Cramer-Rao bound) and the actual variance provided by the estimator when a large data sample is considered. Assume that the constant x is to be estimated by observations of

$$y(t) = x + \eta(t),\ t = 1, 2, \ldots, \bar{N}$$

where $\eta(t)$ is a noise variable. If the noise $\eta(t)$ has a Gaussian distribution, the estimator given by the mean of the observations has an asymptotic efficiency of 1. However, the situation is different if the noise is non-Gaussian, namely when outliers occur. Robust statistics [3] provide methods that are considerably efficient for nonnormal distributions. The literature on time series [4]–[12] and computer vision [13], [14] supplies a *plethora* of such methods and applications. In [15], algorithms for systems identification with data containing outliers are described. However, embedding robust estimation in control (the problem at hand here) received little attention. In [16], predictive adaptive control in the presence of outliers is studied.

Consider now systems where a signal issued by a sensor is fed back to a controller. For tackling sensor faults, the above statistical methods may be used. During the periods in which measurements are not issued by the sensor, control decision must be made on the basis of a plant model used for reconstructing the missing signal. In [17] sufficient conditions for the stability of the closed-loop system under this situation are provided. Two practical problems must be solved:

- detection of the sensor fault occurrence;
- signal reconstruction during the fault.

This paper concerns the referred problems in the context of neuromuscular blockade control of patients undergoing general anaesthesia. The methods considered are general and may, in principle, be used for other types of physiological variables whose measure is prone to transient faults. Several approaches to the neuromuscular blockade control problem as well as an introduction to this issue can be seen in [18]–[25]. Muscle relaxant drugs are frequently given during surgical operations. The nondepolarising types of muscle relaxant act by blocking the neuromuscular transmission (NMT), thereby producing muscle paralysis. The level of muscle relaxation is measured from an evoked

Manuscript received January 16, 2004; revised April 10, 2005. This work was supported in part by the POSI, IIIrd EC Framework Program under project POSI/SRI/39643/2001. The work of H. Magalhães was supported in part by the IIIrd EC Framework Program under the Fundação para a Ciência e Tecnologia (FCT). *Asterisk indicates corresponding author.*

J. M. Lemos and R. Dionísio are with the INESC-ID/IST, 1000-029 Lisboa, Portugal.

H. Magalhães is with the Departamento de Matemática Aplicada, Faculdade de Ciências da Universidade do Porto, 687, 4169-007 Porto, Portugal. He is also with the UI&D Matemática e Aplicações, Universidade de Aveiro, 3810-193Aveiro, Portugal.

*T. Mendonça is with the Departamento de Matemática Aplicada, Faculdade de Ciências da Universidade do Porto, Rua do Campo Alegre, 687, 4169-007 Porto, Portugal. She is also with the UI&D Matemática e Aplicações, Universidade de Aveiro, 3810-193 Aveiro, Portugal (e-mail tmendo@fc.up.pt).

Digital Object Identifier 10.1109/TBME.2005.856259

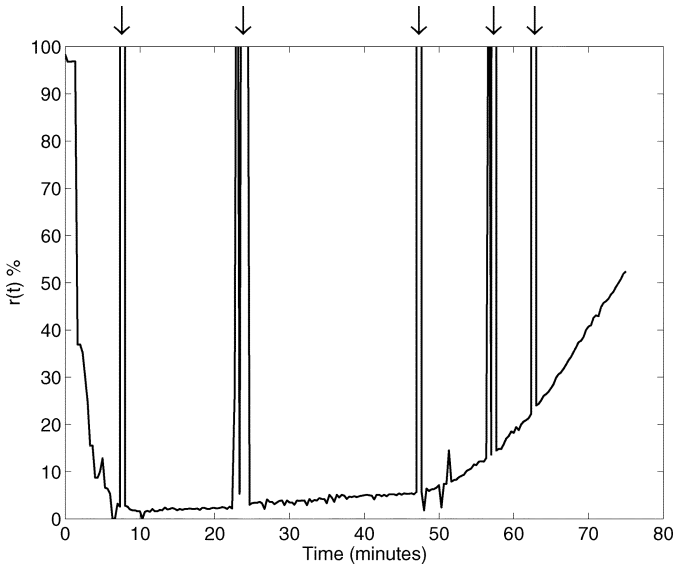

Fig. 1. Occurrence of measurement faults in a neuromuscular blockade record, indicated by arrows. Clinical data obtained with an open-loop system.

EMG at the hand by electrical stimulation of the adductor policies muscle to supramaximal train-of-four stimulation of the ulnar nerve. In a clinical environment the measurement of the neuromuscular blockade level corresponds to the first single response ($T_1\%$) calibrated by a reference twitch, obtained by defining a supramaximal stimulation current. This measurement procedure is prone to failure due to the interaction between technological devices and physiological systems, measurement faults having been reported in practice [24]. These faults manifest themselves as fast changes of the sensor output signal to unrealistic values. Although their cause may be related to a poor electrical coupling between the sensor electrodes and the patient, there are reported cases in which the cause is unknown. Fig. 1 shows one example of the occurrence of measurement faults in a neuromuscular blockade record, obtained in a clinical environment with an open-loop system. The graphic shows the temporal plot of a variable $r(t)$ indicating muscle activity level. For $r(t) = 0\%$ the patient is fully paralyzed while $r(t) = 100\%$ corresponds to normal muscle activity. In the beginning of the surgery, the patient, starting at $r(t) = 100\%$, undergoes a *bolus* of *atracurium*, a drug for inducing neuromuscular blockade. As a consequence, $r(t)$ falls down to a value close to 0%. Then, as the drug is metabolyzed, the variable $r(t)$ gradually increases. Sensor faults are seen as sudden large deviations from a smooth envelope of $r(t)$ and they are indicated in Fig. 1 by arrows.

The contributions of this paper consist in the development and test of sensor signal processing algorithms in order to render control insensitive with respect to the occurrence of sensor faults. These methods are incorporated in an adaptive automatic system [26][1] for feedback control of neuromuscular blockade using continuous infusion of muscle relaxants. A significant contribution consists in the experimental testing of the algorithms in the neuromuscular blockade control of patients undergoing surgery.

[1]The package incorporates a variety of control and filtering techniques and it can be used on patients undergoing surgery or as an advanced simulation tool for education and training purposes.

The paper is organized as follows: after the introduction (Section I), neuromuscular blockade and its control with switched multiple models (Section II) are briefly reviewed in order to recall the aspects which are important for the present framework. The main contributions are contained in Section III, where algorithms for tackling sensor faults are presented. This section includes the results of extensive simulations as well as clinical cases obtained with neuromuscular blockade control. Conclusions are drawn in Section IV.

II. Neuromuscular Blockade Model and Control

This section introduces the model representing the dynamics of neuromuscular blockade and explains the control strategy used.

A. Model

The dynamic response of the neuromuscular blockade for *atracurium* may be modeled as shown in Fig. 2 [23], [27]. A linear pharmacokinetic model (block 1 of Fig. 2), described by the following linear system of state equations:

$$\begin{cases} \dot{x}_1(t) &= -\lambda_1 x_1(t) + a_1 u(t) \\ \dot{x}_2(t) &= -\lambda_2 x_2(t) + a_2 u(t) \\ c_p(t) &= \sum_{i=1}^{2} x_i(t) \end{cases} \tag{1}$$

relates the drug infusion rate $u(t)$ [μg kg^{-1} min^{-1}] with the plasma concentration $c_p(t)$ [μg ml^{-1}], where x_i ($i = 1, 2$) are state variables [implicitly defined by (1)] and a_i [kg ml^{-1}], λ_i [min^{-1}] ($i = 1, 2$) are patient-dependent parameters. The physiological basis of the model described by (1) consists of assuming two plasma compartments (central and peripheric) both communicating with each other. As explained in [28], one decides which class of compartmental model applies from the number of exponential terms (disposition polyexponential equation) needed to describe the plasma concentration-time after intravenous administration. A linear second-order model (blocks 2 and 3 of Fig. 2), described by the cascade of two first-order systems, written as

$$\dot{c}(t) = -\lambda c(t) + \lambda c_p(t) \tag{2}$$

and

$$\dot{c}_e(t) = -\frac{1}{\tau} c_e(t) + \frac{1}{\tau} c(t) \tag{3}$$

is assumed to relate $c_p(t)$ with the concentration in the effect compartment, $c_e(t)$ [μg ml^{-1}]. Here, $c(t)$ is an intermediate variable and λ [min^{-1}], τ [min] are patient-dependent parameters. It is remarked that standard models developed for *atracurium* [29], [30] do not consider the block 3. As shown in [27], the inclusion of the extra delay associated to τ allows a better replication of the observed experimental responses. Finally, the pharmacodynamic effect, that relates $c_e(t)$ to the induced pharmacodynamic response, $r(t)$ [%], may be modeled by the Hill equation [30] (block 4 of Fig. 2)

$$r(t) = \frac{100 C_{50}^{\gamma}}{C_{50}^{\gamma} + c_e^{s}(t)} \tag{4}$$

where the parameters C_{50} [μg ml^{-1}] and γ (adimensional) are also patient-dependent. The variable $r(t)$, normalized between

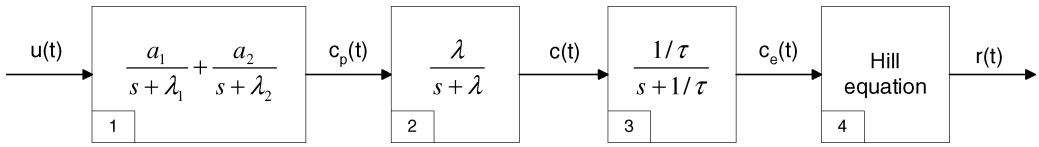

Fig. 2. Block diagram of the neuromuscular blockade model.

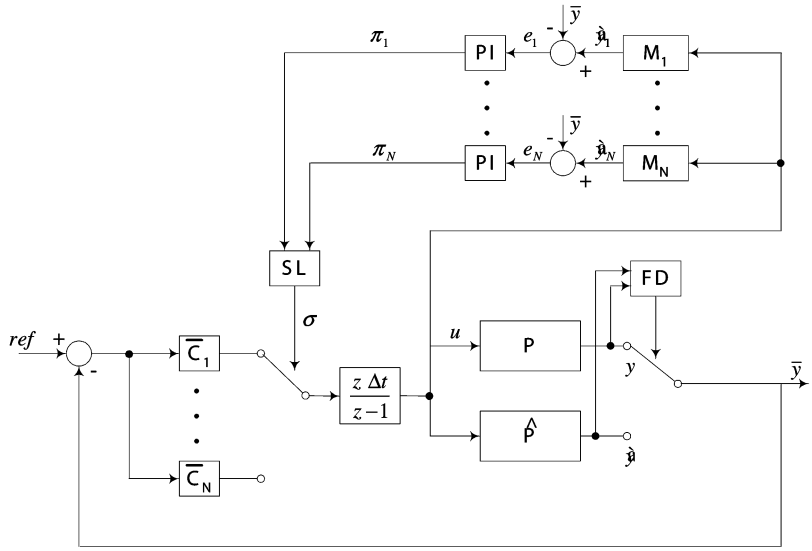

Fig. 3. Modified switched multiple model controller for tackling sensor faults.

0 and 100, measures the level of the neuromuscular blockade, 0 corresponding to full paralysis and 100 to full muscular activity.

The final model for *atracurium* has, therefore, eight parameters [a_1, a_2 [$\mathrm{kg\,ml^{-1}}$], λ_1, λ_2, λ [$\mathrm{min^{-1}}$], τ[min], C_{50} [$\mu\mathrm{g\ ml^{-1}}$], and γ (adimensional)], which (apart from τ following a uniform distribution) follow a multidimensional log-normal probability distribution, as established using statistical methods [27].

B. Control

To achieve a high level of neuromuscular blockade in a short time, a *bolus* of *atracurium* is always administered in the beginning of a surgery. After the administration of the *bolus*, the level of the muscular blockade increases very quickly (the variable r, that measures muscular activity decreases), and full muscle paralysis is induced in a few minutes. Following that initial period, the control objective is to follow a specific reference profile with a final target value $\mathrm{ref} \equiv \mathrm{ref}_0$. The value of the reference profile is initially fixed at a low level (typically 2.5%) during the first 30 min. It is then gradually increased to the final value (typically 10%).

A constant gain digital PID controller incorporating several modifications to accommodate the characteristics of the neuromuscular blockade has been developed in [23]. However, the analysis of a large set of clinical results [23] indicated that the variability of the patient's responses to the infusion of *atracurium* is much greater than that inferred by the data available in the literature [30], therefore suggesting the need for more elaborate control structures.

In order to cover a wide range of behaviors, a family of $N = 100$ nonlinear dynamic models, M_j, $j = 1,\ldots,N$, has been generated using the probabilistic model for *atracurium* discussed previously [27]. For each model M_j, a PID controller C_j, $j = 1,\ldots,N$, has been tuned according to a rule which places a pair of dominant poles [31]. Based on this family of controllers C_j, $j = 1,\ldots,N$, switching multiple model control strategy has been proposed as an alternative method in order to tackle the high degree of uncertainty in neuromuscular blockade model knowledge [32]. The choice $N = 100$ for the number of models/controllers and their distribution was motivated by experimental observations, which suggest that possible outcomes are suitably covered. It is possible to stabilize these bank models with a much smaller number of controllers but, implying a loss of transient performance. Increasing N allows a much closer match between the unknown patient dynamics and the selected controller, according to the adaptive strategy underlying multiple model switching control.

The basic structure of a supervisor based switched multiple model controller including a modification to tackle sensor faults is seen in Fig. 3, as described in [32]–[34]. In Fig. 3, y denotes the sensor measure, $\hat{y}$ denotes an estimate of y free from outliers and $\bar{y}$ is equal to $\hat{y}$ when outliers are detected, being equal to y otherwise. The detection of outliers occurrence is made by the block labeled FD in Fig. 3, to be discussed in the following section. Each C_j of the bank of controllers is designed to match the plant models $M_j, j = 1,\ldots,N$. This set of models is assumed to "cover" all the possibilities of the actual plant P. In order to select at each time which controller best matches P, the principle according to which the best predictive performance model implies the best controller performance is applied.

For evaluating the model predictive performance, the output $\hat{y}_j$, $j = 1, \ldots, N$, of each model M_j is, therefore, compared with the reconstructed output $\bar{y}$ in order to build a prediction error e_j given at each time t by

$$e_j(t) = \hat{y}_j(t) - \bar{y}(t), \quad j = 1, \ldots, N. \tag{5}$$

The performance index (PI) π_j, $j = 1, \ldots, N$, of model j, which provides a measure of the corresponding prediction error power e_j, is computed by low-pass filtering according to

$$\pi_j(t+1) = \lambda_\pi \pi_j(t) + (1 - \lambda_\pi) e_j(t), \quad j = 1, \ldots, N, \tag{6}$$

where t is discrete time and λ_π is a parameter to adjust. The switching logic block SL selects the index σ of the controller to apply to the plant. This selection is given by the value of j corresponding to the least value of π_j, but ensuring that, once a controller is applied to the plant, it remains so for a minimum amount of time τ_D. This is the so called "dwell time" condition, which prevents high frequency commutation among controllers and prevents instabilities that could occur due to too fast switching [33]. An integrator common to all blocks ensures bumpless transfer between different controllers [33] (discrete control transfer function $C_j(z) = \bar{C}_j(z)((z\,\Delta t)/(z-1))$, $j = 1, \ldots, N$).

III. Sensor Faults

Sensor faults correspond to transient periods in which the measure issued by the sensor is not related to the variable to be measured. The class of sensor faults considered in the paper is seen as isolated or repeated (in time) occurrence of outliers. Methods for reconstructing the measured signal in the presence of outliers are now considered.

A. Median Filter

One possibility for modeling sensor faults consists in assuming that the observations y (sensor measures) are obtained by adding to the true value x of the variable a noise η whose probability density function (pdf) is Gaussian

$$p(y \mid x) = \sqrt{\frac{\alpha}{\pi}}\, e^{-\alpha(y-x)^2} \tag{7}$$

but whose inverse variance

$$\alpha = \frac{1}{\sigma_n^2}; \qquad \sigma_n^2 = E[\eta^2(t)] \tag{8}$$

is itself a random variable. By making assumptions with respect to the pdf of α it is possible to model the heavy tails associated with different types of outliers and to deduce algorithms corresponding to these models. Furthermore, by following the approach of [35] it is possible to derive estimation algorithms for x given y from a unified point of view based on loss functions. In the sequel, this approach is used to justify the median filter. It could also be used to derive estimators based on nonquadratic losses, suitable for adaptive self-tuning control in the presence of outliers. However, a different method will be followed leading to algorithms more adequate to combine with switched multiple model control.

Assume that the noise standard deviation is a random variable (r.v.) with pdf

$$p(\sigma_n) = 2\sigma_n e^{-\sigma_n^2/4}. \tag{9}$$

The most likely value of σ_n is close to 1.5. However, higher values of σ_n may also be produced, although with a much lower likelihood, thereby modeling outliers. Let x be the variable to estimate, $\hat{x}$ be its estimate and consider a function $V(\cdot)$ called the loss [2]. The average loss associated to the estimate $\hat{x}$ is defined as

$$J(\hat{x}) = E\left[V(x - \hat{x})\right] \tag{10}$$

where $E[\cdot]$ is the expectation operator. It is shown in [35] that the corresponding loss is the absolute value of the estimation error, instead of its quadratic value as would be the case under Gaussian noise of constant variance. The absolute value is a classical loss function [2], introduced heuristically in order to prevent large deviations of data from distorting the estimate. As is well known [2], the corresponding optimal estimate (minimizing (10) with V given by the absolute value) is the median of the data received. Therefore, the inclusion of a median filter in order to remove outliers from the plant output seems to be adequate. As discussed in [35], other possibilities may be obtained by considering different loss functions V.

Fig. 4 shows a real case of neuromuscular blockade control obtained in a clinical environment. A filter comprising a cascade of a three-point median filter followed by a fifth-order low-pass FIR filter is employed. This is made according to the approach suggested in [36]. As explained above, the median filter cancels the outliers. Once these are eliminated, the high frequency Gaussian noise components are rejected by the FIR filter. The orders have been selected so as to achieve these aims with the introduction of the least possible delay in the signals. The order of the median filter should depend on the duration of the outliers. Longer duration outliers require higher order median filters. Fig. 4(a) shows the sensor output and the upper graphic in Fig. 4(b) shows the filtered signal, while the lower one shows the record of the manipulated variable. At $t = 110$ min the infusion of *atracurium* stops and the muscular activity gradually raises to its normal value. As can be seen in Fig. 4, the major outliers have been filtered out. As will be seen in trials obtained with other methods, an increased tracking performance can be achieved.

B. Bayesian Decision

Another approach for tackling sensor faults is based on Bayesian decision and signal reconstruction. The Bayesian decision procedure detects that a fault has occurred. The sensor output is then replaced by a patient model output selected as detailed later.

In order to explain the Bayesian decision scheme, consider the model generating the faults as shown in Fig. 5. Let $y(t)$ denote the observation made at discrete time t and $x(t)$ be the corresponding true value of the variable to be measured. It is assumed that $x_{\min} \leq x(t) \leq x_{\max}$. Under hypothesis H_0, occurring with probability p_0, close to 1, the observation $y(t)$ is equal to the value of the variable to be measured, $x(t)$, with added zero mean white Gaussian noise of (constant) variance σ_e^2, denoted $e(t)$:

$$y(t) = x(t) + e(t). \tag{11}$$

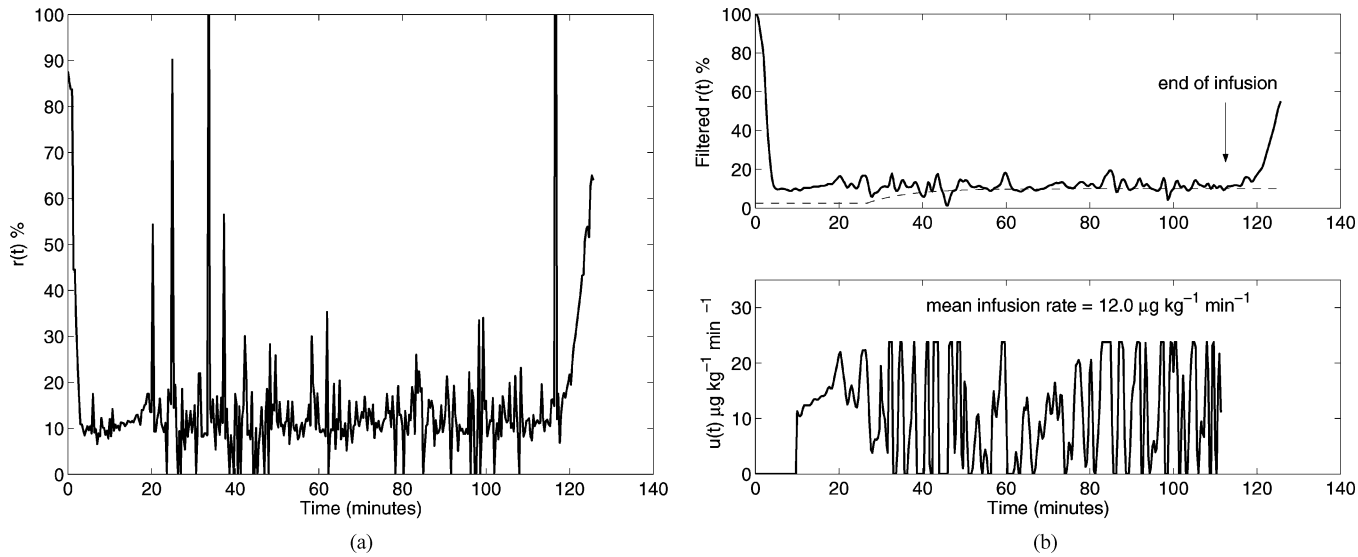

Fig. 4. Clinical results of neuromuscular blockade control obtained with the nonlinear filter comprising a cascade of a three-point median filter followed by a fifth-order low-pass FIR filter. (a) Sensor output and (b) filtered $r(t)$ and control action.

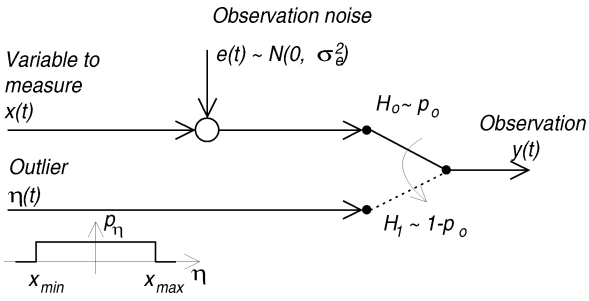

Fig. 5. Model of measurement with interrupted observations.

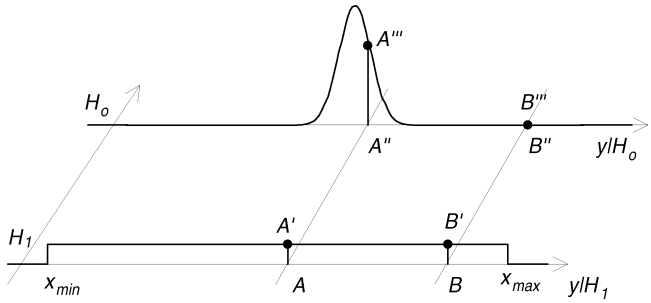

Fig. 6. The pdf of the observations in the presence of interruption measures.

This choice of H_0 corresponds to absence of sensor faults. The sensor output is equal to the variable to be measured corrupted with Gaussian noise which can be attenuated by a linear filter.

Under hypothesis H_1, which occurs with probability $1 - p_0$, close to zero, a measure interruption (sensor fault) occurs. In this case, the observation is no longer related to the variable being measured but, instead, is given by a random variable $\eta(t)$ with a pdf which presents "heavy tails," thereby explaining the frequent occurrence of high values of η. If the signal $x(t)$ to be measured is confined between the values $x_{\min}$ and $x_{\max}$, it is reasonable to assume that the pdf of η is uniform between these two values. The choice of the pdf of η as uniform was made *a priori*, being justified only by the final results obtained in the case of neuromuscular blockade control.

According to a Bayesian approach, in order to detect that a given observation is actually noise, the probability of both hypothesis, given the observations, $P(H_i \mid y(t), Y^{t-1})$ $(i = 0, 1)$, is computed. For H_0 this is

$$P(H_0 \mid y(t), Y^{t-1}) = C \cdot p(y(t) \mid H_0, Y^{t-1}) p_0 \qquad (12)$$

where Y^{t-1} is the set of observations made up to $t-1$, C is a normalizing constant and p_0 is the probability of the occurrence of a nonfaulty measurement (see Fig. 5). Given the model of the observations when H_0 holds, (12) reads

$$P(H_0 \mid y(t), Y^{t-1}) = C \frac{1}{\sigma_e \sqrt{2\pi}} e^{(-(y(t)-x(t))^2/2\sigma_e^2)} p_0. \quad (13)$$

For computing (13), the value of $x(t)$ is needed. Since this is unknown, it is replaced by a convenient estimate $\hat{x}(t)$. To this end, several possibilities may be envisaged as discussed later.

For H_1

$$P(H_1 \mid y(t), Y^{t-1}) = C \frac{1}{x_{\max} - x_{\min}} (1 - p_0) \qquad (14)$$

with C being the same constant as in (13). Both probabilities $P(H_0 \mid y(t), Y^{t-1})$ and $P(H_1 \mid y(t), Y^{t-1})$ are then compared. If

$$\frac{P(H_1 \mid y(t), Y^{t-1})}{P(H_0 \mid y(t), Y^{t-1})} > 1 \qquad (15)$$

it is decided that a sensor fault has occurred. Fig. 6 provides a graphic explanation, showing the pdf of the last observation given each of both hypotheses. If the observation $y(t)$ falls at, say, point *A*, the length of the segment $[A,\ A']$ is smaller than the length of $[A'',\ A''']$ and H_0 is selected. The opposite happens if the observation falls at point *B*, in which H_1 (existence of a measure interruption) is decided. If it is decided that an interruption has occurred, the observation $y(t)$ is discarded and replaced by

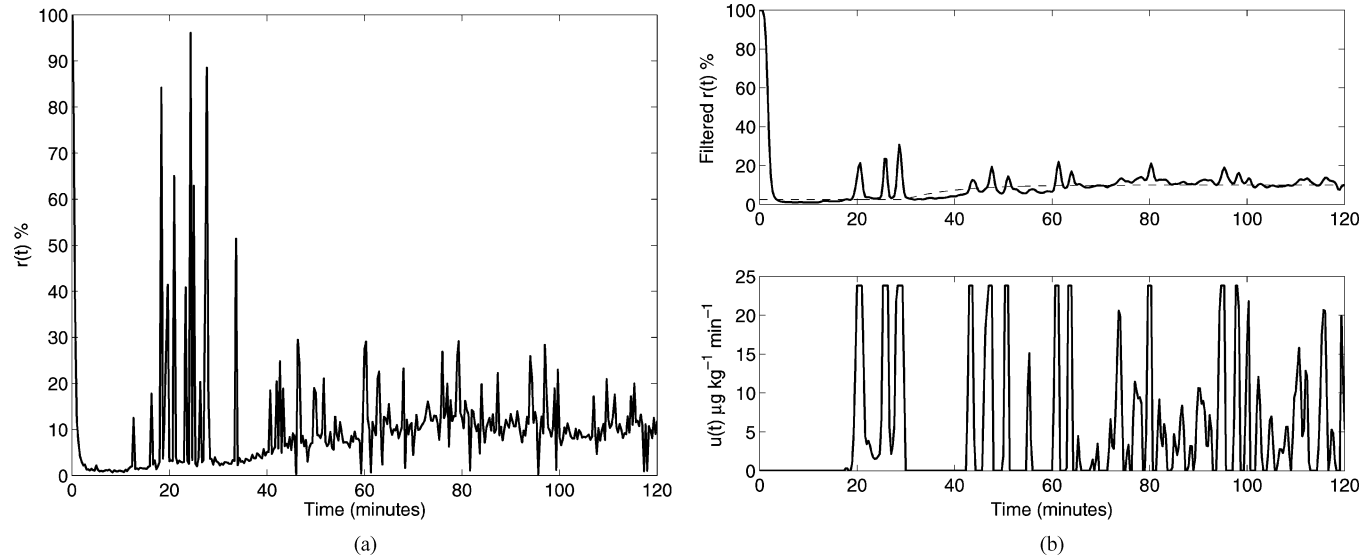

Fig. 7. Simulated results obtained with the nonlinear filter. (a) Sensor output and (b) filtered $r(t)$ and control action.

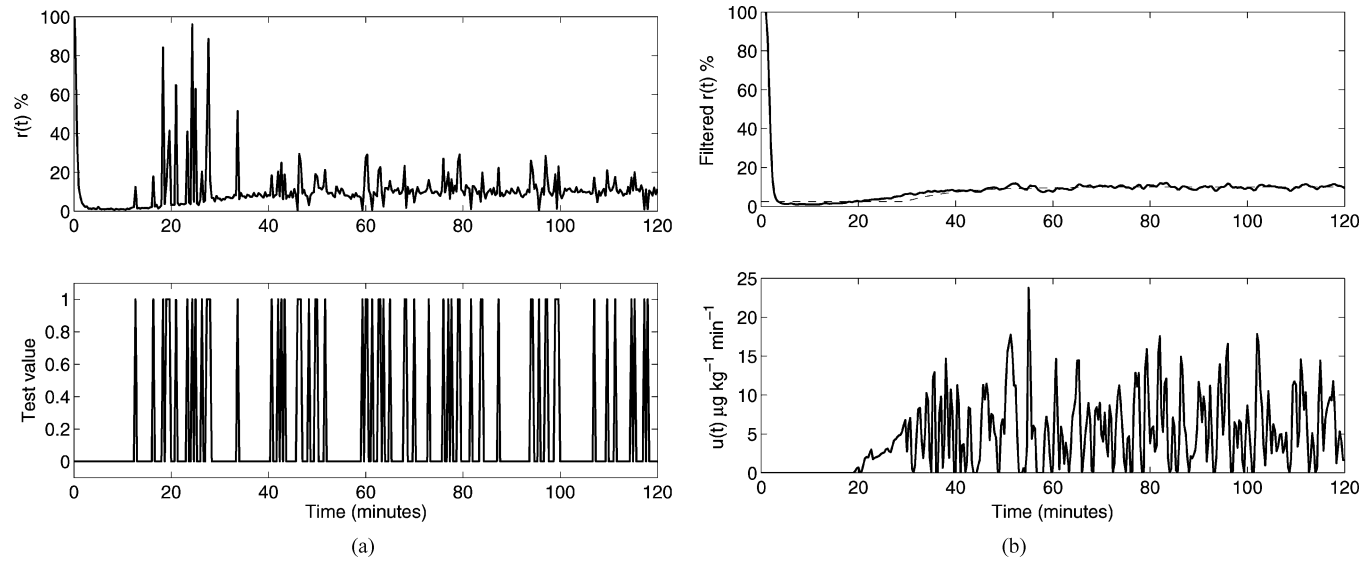

Fig. 8. Simulated results obtained with the Bayesian decision in which the signal is reconstructed using the currently active model from the bank. (a) Sensor output and test value and (b) filtered $r(t)$ and control action.

a forecast $\hat{x}(t)$ of the true value $x(t)$, made from previous observations. Coupling this scheme with switched multiple model control results in the structure of Fig. 3. Here, the fault detection block FD embodies the above mentioned Bayesian decision rule and $\overline{y} = \hat{x}$.

C. Signal Reconstruction

When a fault is detected, the estimate $\hat{x}(t)$ of $x(t)$ cannot be obtained by low-pass filtering of $y(t)$. During these periods, $\hat{x}(t)$ can be generated by a linear system mode, driven by the input $u(t)$ actually applied and defined by an equation of the form

$$\hat{x}(t) = \sum_{i=1}^{p} \gamma_i \hat{x}(t-i) + \sum_{j=1}^{q} \delta_j u(t-j). \tag{16}$$

If switched multiple model control is used, the orders p and q and the coefficients γ_i, δ_j, $i = 1, \ldots, p$, $j = 1, \ldots, q$ are selected as the ones of the closest model of the bank M_j, $j = 1, \ldots, N$, in the sense of minimizing the switched multiple model control performance index. Another possibility is to estimate the coefficients γ_i, δ_j by standard recursive least squares from plant data corresponding to periods in which outliers are not detected. This second possibility will be referred to, hereafter, as the "ARX model," because (16) is the optimal one step ahead predictor associated to an ARX model with the same parameters.

D. Algorithm Comparison

For tackling sensor faults, two possible algorithms are considered.

- Filtering with a combination of a median filter and a FIR filter. This will hereafter be referred for short as "nonlinear filter."

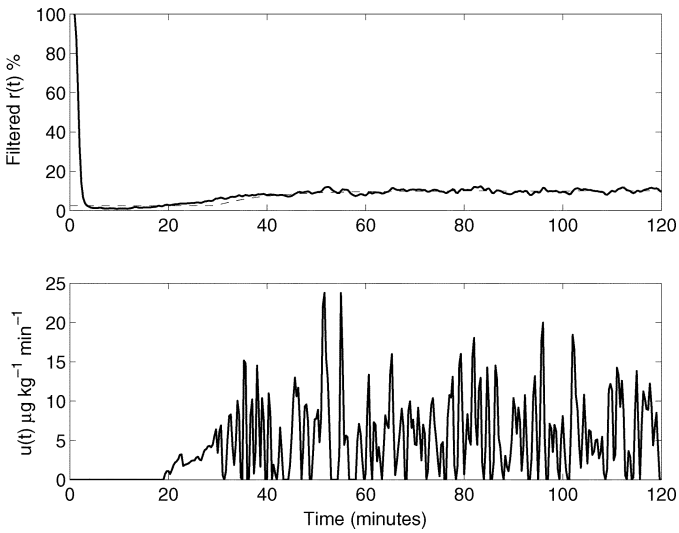

Fig. 9. Simulated results obtained with the Bayesian decision in which the signal is reconstructed using an ARX($p = 6, q = 1$) model (filtered $r(t)$ and control action).

- Filtering with a combination of a Bayesian decision and a FIR filter plus reconstruction. This will hereafter be referred for short as "Bayesian decision".

These two methods are now compared by simulation results. Fig. 7 shows a simulated result that mimics the clinical case (Fig. 4) obtained with the nonlinear filter. The results obtained using Bayesian decision is illustrated in Fig. 8. In this case the control structure of Fig. 3 is used and the signal is reconstructed using the currently active model of the model bank. More specifically, $\hat{P}$ in Fig. 3 is the closest model to data of the model bank M_j, $j = 1, \ldots, N$. Fig. 9 shows the results obtained with Bayesian decision in which the control structure of Fig. 3 is again used, but the signal is now reconstructed using an ARX($p = 6, q = 1$) model whose parameters are recursively estimated on-line. The parameters of the Bayesian decision used are $p_0 = 0.95$ and $\sigma_e^2 = 1.5$. This value of p_0 (used in the algorithm) was intentionally chosen as different from the "true" value used in the model generating the data. In the model, p_0 was made equal to 0.825 for $t < 40$ min and to 0.7 for $t \geq 40$ min. As can be concluded from Figs. 8 and 9, the Bayesian decision leads to a superior performance. From $t = 75$ min (instant at which the reference has already attained the target value [23]) up to the end, the mean square error (MSE) between $r(t)$ and its reference is computed. When the nonlinear filter is used, this index takes the value 4.40. When the Bayesian decision is used and the signal is reconstructed using the currently active model of the model bank, the MSE takes the value 1.91. On the other hand, when the signal is reconstructed using an ARX($p = 6$, $q = 1$) model, the MSE is 2.00. Although these last two results are not significantly different, the method relying on the reconstruction of the signal using ARX models has the disadvantage of having to define the optimal order for the model. By optimal order of the model one means the values of p and q in (16) such that the resulting prediction error power is the least possible.

An important issue to be considered is the degradation of the algorithm performance with the interruption duration. In fact, the interruption can not take too long since the signal is

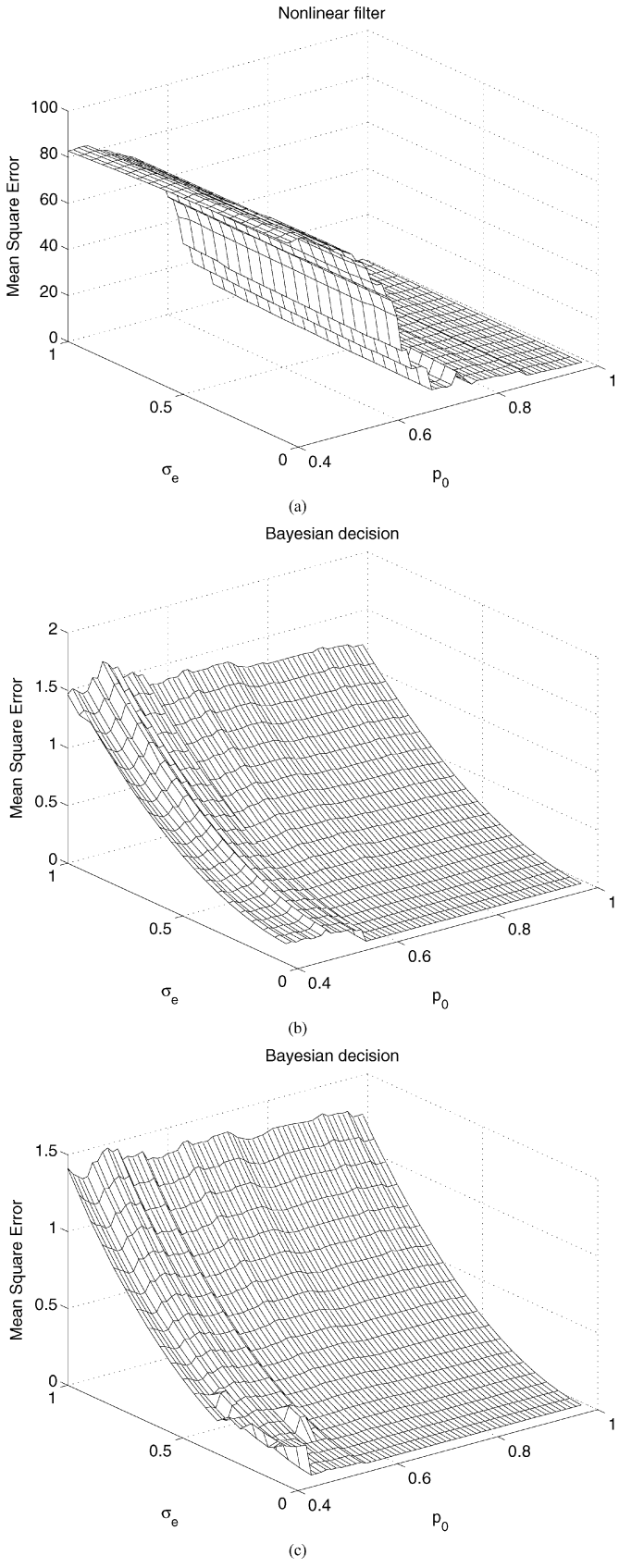

Fig. 10. MSE as a function of σ_e and p_0 in the model generating the data. (a) Nonlinear filter. (b) and (c) Bayesian decision in which the signal is reconstructed using the currently active model from the bank. The parameters of the decision algorithm are (b) $p_0 = 0.95$ and $\sigma_e^2 = 1.5$, (c) $p_0 = 0.8$ and $\sigma_e^2 = 1.5$.

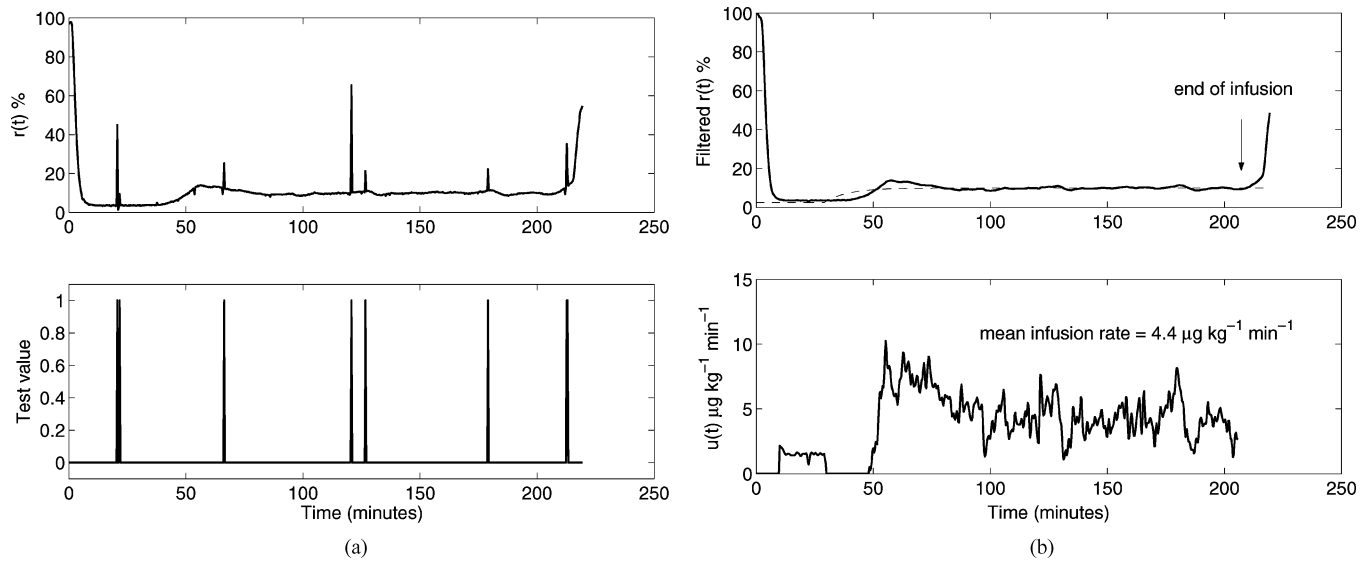

Fig. 11. Clinical results obtained with the Bayesian decision in which the signal is reconstructed using the currently active model from the bank. (a) Sensor output and test value and (b) filtered $r(t)$ and control action.

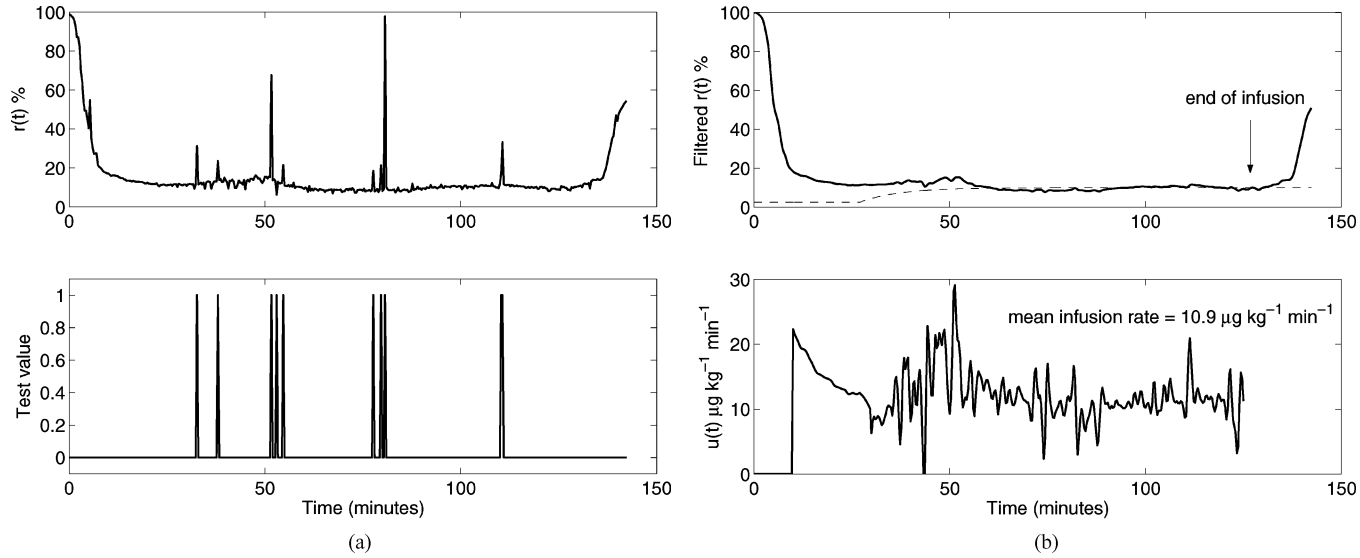

Fig. 12. Clinical results obtained with the Bayesian decision in which the signal is reconstructed using the currently active model from the bank. (a) Sensor output and test value and (b) filtered $r(t)$ and control action.

reconstructed with a model. Fig. 10(a)–(c) shows the MSE as a function of σ_e (Gaussian noise standard deviation) and p_0 (parameters of the model generating the simulated signals) for the nonlinear filter and Bayesian decision in which the signal is reconstructed using the currently active model from the bank. In Fig. 10(b) the parameters of the decision algorithm are kept constant at $p_0 = 0.95$ and $\sigma_e^2 = 1.5$, while in Fig. 10(c), $p_0 = 0.8$ and $\sigma_e^2 = 1.5$. Since $1 - p_0$ is the probability of occurrence of an "outlier" in an isolated sample, smaller values of p_0 correspond, therefore, to an higher probability of longer interruptions. As can be seen by comparing both figures (remark the different scales of the vertical axis), the Bayesian decision leads to much lower values of the average error when p_0 decreases.

E. Clinical Trials

A study was approved by the Ethics Committee of Hospital Geral de Santo António (Porto, Portugal) in order to evaluate and compare the performance of different control strategies including switched multiple model control. At this moment, 30 patients (with health features levels I to IV according to the American Society of Anesthesiology (ASA) have undergone elective surgery with automatic control of neuromuscular blockade. The occurrence of measurement faults have been observed in a reduced number of cases, some of them reported in this paper.

Anesthesia was induced with intravenous *fentanyl* and *propofol*. After calibration of the NMT module [37] of the Datex AS/3 Anaesthesia Monitor (manufactured in Finland), a 500 $\mu\mathrm{gkg}^{-1}\,\mathrm{min}^{-1}$ bolus of *atracurium* was administered. Anesthesia was maintained with *AIR* or $\mathrm{N_2O/O_2}$, *propofol* infusion or *sevoflurane* and *fentanyl* as needed. *Atracurium* $(1\ \mathrm{mg/ml})$ was delivered by a computer controlled syringe driver $(\mathrm{B|Braun\ Perfusor\ compact\ S}$ [38]). The controller is implemented in a portable battery operated computer that

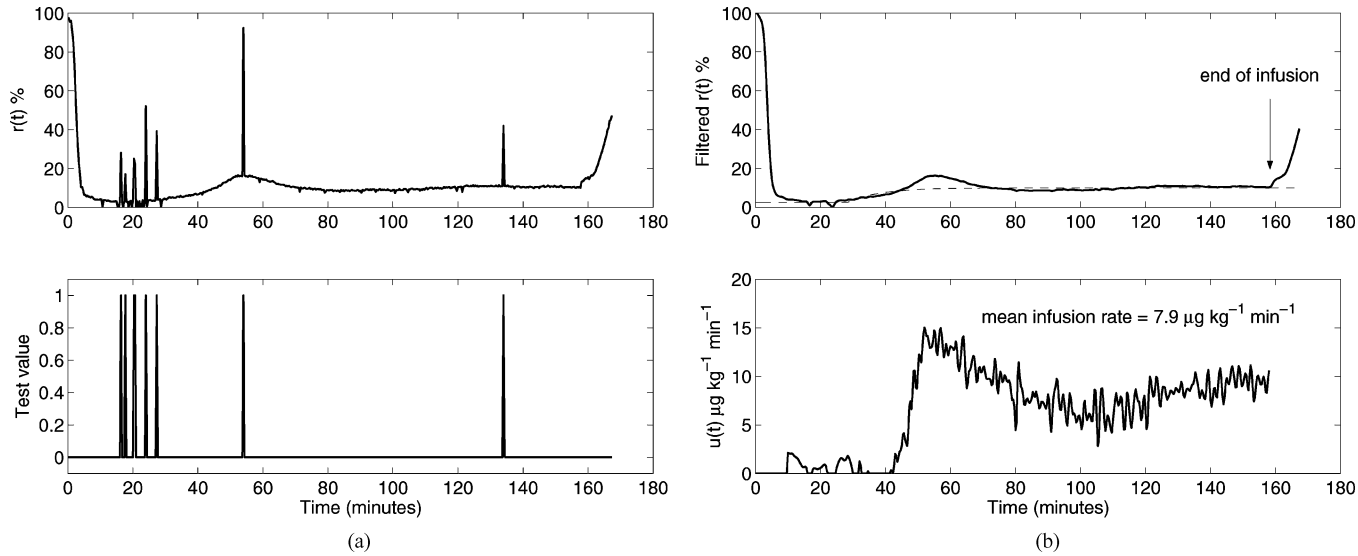

Fig. 13. Clinical results obtained with the Bayesian decision in which the signal is reconstructed using the currently active model from the bank. (a) Sensor output and test value and (b) filtered $r(t)$ and control action.

receives the $T_1\%$ signal (via RS 232C) from the Datex AS/3 and updates the infusion rate delivered by the pump every 20 s.

Fig. 11 shows a clinical result obtained with the Bayesian decision in which the signal is reconstructed using the currently active model of the model bank. The upper graphic in Fig. 11(a) shows the sensor output, while the lower one shows the test value. The test value is a variable which assumes the value 1 when an outlier is detected, i.e., when (15) holds, being zero otherwise. In Fig. 11(b), the upper graphic shows the filtered signal, while the lower one shows the manipulated variable. The vertical arrow indicates the end of the infusion, when the control system is disconnected. The parameters of the bayesian filter used are $p_0 = 0.95$ and $\sigma_e^2 = 3$. This choice was made on the basis of simulation in order to get a compromise between good detection and false alarms. As can be seen in Fig. 11, the outliers have been removed and the resulting performance of this strategy is good ($\mathrm{MSE} = 0.38$).

Fig. 12 shows the results of a different clinical trial, the parameters of the decision algorithm being the same as in the previous case. Although the initial *bolus* was insufficient to drive $r(t)$ close to zero, when the controller was connected it was able to track the reference ($\mathrm{MSE} = 0.89$).

In Fig. 13 the results of another clinical trial are shown, the parameters of the decision algorithm being the same as in the previous cases. Despite the initial overshoot ($r(t) \approx 16.5\%$), the controller maintained the desired reference throughout the surgery ($\mathrm{MSE} = 0.75$).

IV. Conclusion

The problem of embedding sensor fault tolerance in feedback control of physiological variables is considered from a unified point of view. The presence of outliers due to sensor faults in the feedback signal entering the controller causes a degradation of tracking performance. Indeed, outliers will be seen as disturbances (actually not existing) to which the controller will react. Outliers can be removed by a median filter. However, for longer duration sensor faults, the median filter is no longer effective and the output signal has to be reconstructed during the periods in which it is missing. A structure relying on Bayesian inference and a predictive filter is proposed. The above algorithms are illustrated by simulations and clinical results using the control of neuromuscular blockade as a case study.

Acknowledgment

The authors would like to thank the referees for their comments, which helped them to improve this paper.

References

[1] A. Rencher, *Multivariate Statistical Inference and Applications*. New York: Wiley Interscience, 1998.
[2] H. V. Trees, *Detection, Estimation, and Modulation Theory, Part I*. New York: Wiley, 1967.
[3] P. Huber, *Robust Statistics*. New York: Wiley, 1981.
[4] K. Boyer and T. Ozguner, "Robust online detection of pipeline corrosion from range data," *Mach. Vis. Applicat.*, vol. 12, no. 6, pp. 291–304, 2001.
[5] J. Dunagan and S. Vempala, "Optimal outlier removal in high-dimensional spaces," *J. Comput. Syst. Sci.*, vol. 68, no. 2, pp. 335–373, 2004.
[6] L. Fahrmeier and R. Künstler, "Penalized likelihood smoothing in robust state space models," *Metrika*, vol. 49, no. 3, pp. 173–191, 1999.
[7] R. Ganguli, "Noise and outlier removal from jet engine health signals using weighted FIR median hybrid filters," *Mech. Syst. Signal Process.*, vol. 16, no. 6, pp. 967–978, 2002.
[8] P. Groot, G. Postma, W. Melssen, L. Buydens, V. Deckert, and R. Zenobi, "Application of principal component analysis to detect outliers and spectral deviations in near-field surface enhanced Raman spectra," *Analytica Chimica Acta.*, vol. 446, no. 1-2, pp. 71–83, 2001.
[9] M. Imhoff, M. Bauer, U. Gather, and D. Löhlein, "Statistical pattern detection in univariate time series of intensive care on-line monitoring data," *Intensive Care Med.*, vol. 24, no. 12, pp. 1305–1314, 1998.
[10] G. Ljung, "On outlier detection in time series," *J. Roy. Statist. Soc.*, ser. B, vol. 55, pp. 559–567, 1993.
[11] S. Mertikas and C. Rizos, "On-line detection of abrupt changes in the carrier-phase measurements of GPS," *J. Geodesy*, vol. 71, no. 8, pp. 469–482, 1997.
[12] R. Taplin and A. Raftery, "Analysis of agricultural field trials in the presence of outliers and fertility jumps," *Biometrics*, vol. 50, pp. 764–781, 1994.
[13] A. Dante and M. Brookes, "Precise real-time outlier removal from motion vector fields for 3-D reconstruction," in *Proc. Int. Conf. Image Processing*, vol. 1, 2003, pp. 393–396.

[14] P. Meer, D. Mintz, and A. Rosenfeld, "Robust regression methods for computer vision: A review," *Int. J. Comput. Vis.*, vol. 6, no. 1, pp. 59–70, 1991.
[15] R. Pearson, "Outliers in process modeling and identification," *IEEE Trans. Contr. Syst. Technol.*, vol. 10, no. 1, pp. 55–63, Jan. 2002.
[16] J. M. Lemos, R. Silva, and J. Marques, "Adaptive control of the ball and beam plant in the presence of sensor measure outliers," in *Proc. American Control Conference (ACC'02)*, Anchorage, AK, 2002.
[17] R. Dionísio and J. M. Lemos, "Stability results for discrete systems controlled in the presence of interrupted observations," presented at the 11th Mediterranean Conf. Control and Automation (MED'03), Rhodes, Greece, Jun. 2003.
[18] R. Jaklitsch and D. Westenskow, "A model-based self-adjusting two-phase controller for *vecuronium*-induced muscle relaxation during anesthesia," *IEEE Trans. Biomed. Eng.*, vol. BME-34, pp. 583–594, 1987.
[19] M. Kansanaho and K. Olkkola, "Performance assessment of an adaptive model-based feedback controller: Comparison between *atracurium*, *mivacurium*, *rocuronium* and *vecuronium*," *J. Clin. Monitor. Comput.*, vol. 13, no. 4, pp. 217–224, 1996.
[20] D. Linkens, *Intelligent Control in Biomedicine*. Lomdon, U.K.: Taylor and Francis, 1994.
[21] D. Mason, N. Edwards, D. Linkens, and C. Reilly, "Performance assessment of a fuzzy controller for *atracurium* induced neuromuscular block," *Br. J. Anaesth.*, vol. 76, no. 3, pp. 396–400, 1996.
[22] D. Mason, J. Ross, N. Edwards, D. Linkens, and C. Reilly, "Self-learning fuzzy control with temporal knowledge for *atracurium*-induced neuromuscular block during surgery," *Comput. Biomed. Res.*, vol. 32, no. 3, pp. 187–197, 1999.
[23] T. Mendonça and P. Lago, "PID control strategies for the automatic control of neuromuscular blockade," *Contr. Eng. Practice*, vol. 6, no. 10, pp. 1225–1231, 1998.
[24] J.-S. Shieh, S.-Z. Fan, L.-W. Chang, and C.-C. Liu, "Hierarchical rule-based monitoring and fuzzy logic control for neuromuscular block," *J. Clin. Monitor. Comput.*, vol. 16, no. 8, pp. 583–592, 2000.
[25] C. Wait, V. Goat, and C. Blogg, "Feedback control of neuromuscular blockade: A simple system for infusion of *atracurium*," *Anaesthesia*, vol. 42, no. 11, pp. 1212–1217, 1987.
[26] H. Magalhães, T. Mendonça, and P. Lago, "A MATLAB smart adaptive system for the control of neuromuscular blockade," in *Proc. 2nd Eur. Medical & Biological Engineering Conf. (EMBEC'02)*, Vienna, Austria, Dec. 2002, pp. 664–665.
[27] P. Lago, T. Mendonça, and L. Gonçalves, "On-line autocalibration of a PID controller of neuromuscular blockade," in *Proc. 1998 IEEE Int. Conf. Control Applications*, Trieste, Italy, Sep. 1998, pp. 363–367.
[28] G. Tucker, "Pharmacokinetic models – Different approaches," in *Quantitation, Modeling and Control in Anaesthesia*, H. Stoeckel, Ed. Stuttgart, Germany: Georg Thieme Verlag, 1985, ch. 2, pp. 54–64.
[29] S. Ward, E. Neill, B. Weatherley, and I. Corall, "Pharmacokinetics of *atracurium* besylate in healthy patients (after a single i.v. *bolus* dose)," *Br. J. Anaesth.*, vol. 55, no. 2, pp. 113–118, 1983.
[30] B. Weatherley, S. Williams, and E. Neill, "Pharmacokinetics, pharmacodynamics and dose-response relationships of *atracurium* administered i. v.," *Br. J. Anaesth.*, vol. 55, pp. 39s–45s, 1983.
[31] K. Åström and T. Hägglund, *Automatic Tuning of PID Controllers*. Research Triangle, NC: Instrument Society of America, 1988.
[32] T. Mendonça, P. Lago, H. Magalhães, A. Neves, and P. Rocha, "On-line multiple model switching control implementation: A case study," presented at the 10th Mediterranean Conf. Control and Automation (MED'02), Lisbon, Portugal, Jul. 2002.
[33] S. Morse, "Supervisory control of families of linear set-point controllers—Part 1: Exact matching," *IEEE Trans. Automat. Contr.*, vol. 41, no. 10, pp. 1413–1431, Oct. 1996.
[34] K. Narendra and J. Balakrishnan, "Adaptive control using multiple models," *IEEE Trans. Automat. Contr.*, vol. 42, no. 2, pp. 171–187, Feb. 1997.
[35] F. Girosi, "Models of Noise and Robust Estimates," MIT, Artificial Intelligence Laboratory, Cambridge, MA, Tech. Rep. Memo no. 1287, 1991.
[36] L. Rabiner, M. Sambur, and C. Schmidt, "Applications of a nonlinear smoothing algorithm to speech processing," *IEEE Trans. Acoust., Speech, Signal Process.*, vol. ASSP-23, no. 6, pp. 552–557, Dec. 1975.
[37] The Datex-Ohmeda Website [Online]. Available: http://www.datex-ohmeda.com /clinical/ cw_prev_01_article5.htm
[38] The B|BRAUN Website [Online]. Available: http://www.bbraunusa.com/ products/ infusion/perfusor_cl.html

João M. Lemos (M'89) received the Ph.D. degree from the Instituto Superior Técnico (IST), Technical University of Lisbon, Portugal, in 1989.

After extensive periods of research work at the University of Florence, Italy, he became Associate Professor in 1997. Currently, he is full Professor of Automatic Control at IST and researcher of INESC-ID, where he leads the Control of Dynamic Systems Group since 1989. He co-authored 31 journal papers and book chapters and 115 conference (peer reviewed) papers, and supervised six Ph.D. degree theses (completed). His research interests are in the area of computer control including, in particular, adaptive predictive control, modeling and identification, and process monitoring using stochastic methods, and control of hyperbollic distributed parameter systems. He has been involved, both either as responsible or participant, in applications to industrial processes, large-scale boilers in thermoelectric plants, solar collector fields, biomedical systems, and biochip temperature control.

Hugo Magalhães was born in Porto, Portugal, in 1979. He received a four-year degree in applied mathematics to technology from Faculdade de Ciências da Universidade do Porto (FCUP), Portugal, in 2001. He is currently working towards the Ph.D. degree in the Department of Applied Mathematics at FCUP, supported by Fundação para a Ciência e Tecnologia (FCT), IIIrd EC Framework Program, under the subject: Adaptive Control: methods and applications. He also incorporates the Mathematical Systems Theory Group from the research and development unit UI&D Matemática e Aplicações, Universidade de Aveiro, Portugal. His research interests include robust adaptive control and switching control, in particular applied to biomedical systems.

Mr. Magalhães received the Eng. António de Almeida prize for best student.

Teresa Mendonça (M'03) was born in Porto, Portugal. She received the applied mathematics degree and the Ph.D. degree in applied mathematics (systems theory and signal processing) from Faculdade de Ciências da Universidade do Porto (FCUP), Portugal, in 1993.

She is currently an Auxiliar Professor in the Department of Applied Mathematics at FCUP and Researcher in the Mathematical Systems Theory Group, UI&D Matemática e Aplicações, Universidade de Aveiro, Portugal. Her research interests are in the area of control systems, in particular. applied to biomedical systems. She has been involved in projects on modeling and control of anaesthesia area.

Rui Dionísio was born in Lisbon, Portugal, in 1968. He received the electrical engineering degree and the M.Sc. degree in electrical engineering from the Lisbon Technical University, Technical Superior Institute, Lisbon, in 1991 and 1996, respectively. He is currently working towards the Ph.D. degree in electrical engineering at the Lisbon Technical University, in the field of adaptive predictive fault-tolerant control.

Currently, he is Adjoint Professor at the Escola Superior de Tecnologia, Instituto Politécnico de Setúbal, where he teaches industrial instrumentation subjects.